Photonic crystal nanocavities fabricated from chalcogenide glass fully embedded in an index-matched cladding with a high Q-factor (>750,000)

Xin Gai,[1,*] Barry Luther-Davies,[1] and Thomas P. White[1,2]

[1]*Centre for Ultrahigh-bandwidth Devices for Optical Systems (CUDOS), Laser Physics Centre, Research School of Physics and Engineering, Australian National University, Canberra, ACT 2600, Australia*
[2]*Centre for Sustainable Energy Systems, Research School of Engineering, Australian National University, Canberra, ACT 2600, Australia*
[*]*xga111@rsphysse.anu.edu.au*

Abstract: We have designed and fabricated a 2-D photonic crystal hetero-structure cavity in the chalcogenide glass $Ge_{11.5}As_{24}Se_{64.5}$ that is fully embedded in a cladding with refractive index of 1.44. The low index contrast of this structure (≈1.21) means that high-Q resonances cannot be obtained using standard hetero-structure cavity designs based on W1 waveguides. We show that reducing the waveguide width can substantially improve light confinement, leading to high-Q resonances in a hetero-structure cavity. Numerical simulations indicate intrinsic $Q_v > 10^7$ are possible with this approach. Experimentally, an optical cavity with a high intrinsic $Q_v > 7.6 \times 10^5$ was achieved in a structure with a theoretical $Q_v = 1.7 \times 10^6$.

OCIS codes: (130.5296) Photonic crystal waveguides; (160.2750) Glass and other amorphous materials; (220.4241) Nanostructure fabrication; (230.5750) Resonators.

References and links

1. S. G. Johnson, S. H. Fan, P. R. Villeneuve, J. D. Joannopoulos, and L. A. Kolodziejski, "Guided modes in photonic crystal slabs," Phys. Rev. B **60**(8), 5751–5758 (1999).
2. S. G. Johnson, P. R. Villeneuve, S. H. Fan, and J. D. Joannopoulos, "Linear waveguides in photonic-crystal slabs," Phys. Rev. B **62**(12), 8212–8222 (2000).
3. J. D. Joannopoulos, S. G. Johnson, J. N. Winn, and R. D. Meade, *Photonic Crystals: Molding the Flow of Light* (Princeton University Press, 2008).
4. T. Baba, "Slow light in photonic crystals," Nat. Photonics **2**(8), 465–473 (2008).
5. T. Baba and D. Mori, "Slow light engineering in photonic crystals," J. Phys. D Appl. Phys. **40**(9), 2659–2665 (2007).
6. C. M. de Sterke, J. Walker, K. B. Dossou, and L. C. Botten, "Efficient slow light coupling into photonic crystals," Opt. Express **15**(17), 10984–10990 (2007).
7. C. Monat, M. Spurny, C. Grillet, L. O'Faolain, T. F. Krauss, B. J. Eggleton, D. Bulla, S. Madden, and B. Luther-Davies, "Third-harmonic generation in slow-light chalcogenide glass photonic crystal waveguides," Opt. Lett. **36**(15), 2818–2820 (2011).
8. B. Corcoran, C. Monat, C. Grillet, D. J. Moss, B. J. Eggleton, T. P. White, L. O'Faolain, and T. F. Krauss, "Green light emission in silicon through slow-light enhanced third-harmonic generation in photonic-crystal waveguides," Nat. Photonics **3**(4), 206–210 (2009).
9. C. Monat, C. Grillet, B. Corcoran, D. J. Moss, B. J. Eggleton, T. P. White, and T. F. Krauss, "Investigation of phase matching for third-harmonic generation in silicon slow light photonic crystal waveguides using Fourier optics," Opt. Express **18**(7), 6831–6840 (2010).
10. H. Oda, K. Inoue, Y. Tanaka, N. Ikeda, Y. Sugimoto, H. Ishikawa, and K. Asakawa, "Self-phase modulation in photonic-crystal-slab line-defect waveguides," Appl. Phys. Lett. **90**(23), 231102 (2007).
11. K. Suzuki, Y. Hamachi, and T. Baba, "Fabrication and characterization of chalcogenide glass photonic crystal waveguides," Opt. Express **17**(25), 22393–22400 (2009).
12. J. F. McMillan, M. B. Yu, D. L. Kwong, and C. W. Wong, "Observation of four-wave mixing in slow-light silicon photonic crystal waveguides," Opt. Express **18**(15), 15484–15497 (2010).

#168795 - $15.00 USD Received 17 May 2012; revised 18 Jun 2012; accepted 21 Jun 2012; published 25 Jun 2012

13. C. Monat, M. Ebnali-Heidari, C. Grillet, B. Corcoran, B. J. Eggleton, T. P. White, L. O'Faolain, J. Li, and T. F. Krauss, "Four-wave mixing in slow light engineered silicon photonic crystal waveguides," Opt. Express **18**(22), 22915–22927 (2010).
14. V. Eckhouse, I. Cestier, G. Eisenstein, S. Combrié, P. Colman, A. De Rossi, M. Santagiustina, C. G. Someda, and G. Vadalà, "Highly efficient four wave mixing in GaInP photonic crystal waveguides," Opt. Lett. **35**(9), 1440–1442 (2010).
15. Y. Akahane, T. Asano, B. S. Song, and S. Noda, "High-Q photonic nanocavity in a two-dimensional photonic crystal," Nature **425**(6961), 944–947 (2003).
16. B. S. Song, S. Noda, T. Asano, and Y. Akahane, "Ultra-high-Q photonic double-heterostructure nanocavity," Nat. Mater. **4**(3), 207–210 (2005).
17. Y. Akahane, T. Asano, B. S. Song, and S. Noda, "Fine-tuned high-Q photonic-crystal nanocavity," Opt. Express **13**(4), 1202–1214 (2005).
18. M. W. Lee, C. Grillet, C. Monat, E. Mägi, S. Tomljenovic-Hanic, X. Gai, S. Madden, D. Y. Choi, D. Bulla, B. Luther-Davies, and B. J. Eggleton, "Photosensitive and thermal nonlinear effects in chalcogenide photonic crystal cavities," Opt. Express **18**(25), 26695–26703 (2010).
19. M. Notomi, A. Shinya, S. Mitsugi, G. Kira, E. Kuramochi, and T. Tanabe, "Optical bistable switching action of Si high-Q photonic-crystal nanocavities," Opt. Express **13**(7), 2678–2687 (2005).
20. T. Tanabe, M. Notomi, S. Mitsugi, A. Shinya, and E. Kuramochi, "Fast bistable all-optical switch and memory on a silicon photonic crystal on-chip," Opt. Lett. **30**(19), 2575–2577 (2005).
21. M. K. Kim, I. K. Hwang, S. H. Kim, H. J. Chang, and Y. H. Lee, "All-optical bistable switching in curved microfiber-coupled photonic crystal resonators," Appl. Phys. Lett. **90**(16), 161118 (2007).
22. M. Dinu, F. Quochi, and H. Garcia, "Third-order nonlinearities in silicon at telecom wavelengths," Appl. Phys. Lett. **82**(18), 2954–2956 (2003).
23. A. D. Bristow, N. Rotenberg, and H. M. van Driel, "Two-photon absorption and Kerr coefficients of silicon for 850-2200 nm," Appl. Phys. Lett. **90**(19), 191104 (2007).
24. C. Quémard, F. Smektala, V. Couderc, A. Barthelemy, and J. Lucas, "Chalcogenide glasses with high non linear optical properties for telecommunications," J. Phys. Chem. Solids **62**(8), 1435–1440 (2001).
25. J. M. Harbold, F. O. Ilday, F. W. Wise, and B. G. Aitken, "Highly nonlinear Ge-As-Se and Ge-As-S-Se glasses for all-optical switching," IEEE Photon. Technol. Lett. **14**(6), 822–824 (2002).
26. A. Prasad, C. J. Zha, R. P. Wang, A. Smith, S. Madden, and B. Luther-Davies, "Properties of $Ge_xAs_ySe_{1-x-y}$ glasses for all-optical signal processing," Opt. Express **16**(4), 2804–2815 (2008).
27. D. J. Lockwood and L. Pavesi, *Silicon Photonics* (Springer-Verlag, 2004).
28. M. Schaub, J. Schwiegerling, E. C. Fest, A. Symmons, and R. H. Shepard, *Molded Optics: Design and Manufacture* (CRC Press, 2011).
29. D. Freeman, S. Madden, and B. Luther-Davies, "Fabrication of planar photonic crystals in a chalcogenide glass using a focused ion beam," Opt. Express **13**(8), 3079–3086 (2005).
30. M. W. Lee, C. Grillet, S. Tomljenovic-Hanic, E. C. Mägi, D. J. Moss, B. J. Eggleton, X. Gai, S. Madden, D. Y. Choi, D. A. Bulla, and B. Luther-Davies, "Photowritten high-Q cavities in two-dimensional chalcogenide glass photonic crystals," Opt. Lett. **34**(23), 3671–3673 (2009).
31. R. J. M. Palma, T. E. Clark, and C. G. Pantano, "Fabrication of two-dimensional photonic crystals in a chalcogenide glass," Int. J. Nanotechnol. **6**(12), 1113–1120 (2009).
32. S. W. Jeon, J. K. Han, B. S. Song, and S. Noda, "Glass-embedded two-dimensional silicon photonic crystal devices with a broad bandwidth waveguide and a high quality nanocavity," Opt. Express **18**(18), 19361–19366 (2010).
33. X. Gai, S. Madden, D. Y. Choi, D. Bulla, and B. Luther-Davies, "Dispersion engineered $Ge_{11.5}As_{24}Se_{64.5}$ nanowires with a nonlinear parameter of 136 $W^{-1}m^{-1}$ at 1550 nm," Opt. Express **18**(18), 18866–18874 (2010).
34. X. Gai, D.-Y. Choi, S. Madden, and B. Luther-Davies, "Polarization-independent chalcogenide glass nanowires with anomalous dispersion for all-optical processing," Opt. Express **20**(12), 13513–13521 (2012).

1. Introduction

Slab photonic crystal (PhC) waveguides, which utilize the band gap of a periodic structure to confine light in the horizontal direction whilst guiding light vertically by total internal reflection, have great potential for all-optical processing. In particular, their small footprint makes them easy to integrate to create compact devices whilst their strong light confinement leads to high light intensities that enhance the nonlinear response [1–3]. The intensity can be further increased through the use of slow light propagation [4–6] or resonant enhancement in cavities. Slow light enhanced nonlinear processing has been demonstrated in PhC waveguides in a range of materials, utilizing third harmonic generation for all-optical pulse monitoring [7–9]; self-phase modulation [10]; and FWM [11–14]. The second way of enhancing the nonlinear response is to incorporate a PhC micro-cavity to confine the light spatially and temporally. This is particularly promising for compact switching devices operating with

#168795 - $15.00 USD Received 17 May 2012; revised 18 Jun 2012; accepted 21 Jun 2012; published 25 Jun 2012

exceptionally low power. It is this second opportunity that we explore in this work. High quality PhC resonant cavities have already been reported in silicon membranes achieving Q factors ranging from 10^5 to 10^6. Examples are the "L3" micro-cavities created by removing 3 holes from a periodic structure [15] and hetero-structures that create mirrors by shifting the dispersion curve of the guided mode by varying the lattice constant along the waveguide [16].

One of the most interesting phenomena achievable in a photonic crystal resonant cavity is bistable switching which would be very useful for all-optical signal processing at low powers. Much effort has been expended to generate high Q resonant cavities with minimum mode volume to achieve ultra-fast bistable switching by the nonlinear Kerr effect [15, 17]. However, so far most experiments on switching have been dominated by thermal nonlinearities [18, 19], or those induced by two-photon absorption (TPA) and free carrier generation [20, 21] and thus have slower recovery times. The fastest bistable switching that has been achieved in a silicon photonic crystal used free carrier nonlinearities and had a relaxation time of over 100ps which is far below the requirement for ultrafast all-optical processing [20, 21]. It must be noted that resonant cavities inevitably reduce the response time even for ultrafast Kerr switching, however, by choosing a moderate Q (<10,000) switching on the <20ps timescale should still be achievable.

Thus, we have been seeking solutions for photonic crystals that can decrease the role of thermal nonlinear effects as well as TPA and free-carrier absorption (FCA) with the aim of achieving switching from the Kerr nonlinearity alone. As a semiconductor, silicon shows significant TPA and FCA effects [22, 23] and hence our approach has been to replace the silicon with a chalcogenide glass in which TPA and FCA can be negligible [24–26]. The magnitude of the thermal nonlinear effect, however, is determined by the linear absorption in the photonic crystal waveguide and the thermo-optic coefficient, dn/dt, of the material. Because the thermo-optic coefficient of the chalcogenides is similar to silicon [27, 28], it is difficult to reduce the thermal nonlinearity by simply changing the slab material. However, in most previous work, the photonic crystal structures have been fabricated as air-suspended membranes to maximize the vertical index contrast, and thus reduce coupling between the guided modes of the PhC slab and radiation modes above the light line [1–3, 29–31]. However, air has very poor thermal conduction, leading a low threshold for the thermal nonlinearity and a very slow recovery time for thermal switching. As a result, we need to design a structure that has much better cooling since this will increase the threshold for the thermal nonlinearity.

Thus, although we cannot reduce dn/dt by changing the slab material, we can reduce the temperature rise, ΔT, by improving heat conduction from the slab, for example, by applying a solid cladding. A solid cladding also provides the opportunity to make an athermal structure if we can find a cladding whose thermo-optic coefficient has the opposite sign and an appropriate magnitude compared with the slab. For example, most polymers or liquids have a negative thermo-optic coefficient compared with chalcogenide glasses for which it is positive.

The addition of a cladding, however, reduces the index contrast drastically and this severely restricts the bandwidth of the guided modes under the light line. This makes it difficult to find a structure that can support a high Q resonance. Even for a silicon PhC embedded in a spin-on glass cladding, the bandwidth was less than 20nm for a W1 waveguide and a Q-factor of only 1.6×10^5 was achieved in a heterostrucure cavity whose Q was predicted to be 2×10^5 [32]. Because chalcogenide glasses have a smaller refractive index than silicon, chalcogenide PhCs will suffer a more severe bandwidth restriction compared with silicon and this implies an even lower Q-factor. Another challenge is that the fabrication process for chalcogenide glass photonic crystals is less mature than for silicon and presents additional difficulties because the glass is relatively soft and fragile.

In this paper, we summarize work on the design and fabrication of high quality photonic crystals from the photo-stable chalcogenide glass $Ge_{11.5}As_{24}Se_{64.5}$ [26, 33, 34] using electron-beam lithography and dry etching [33, 34]. To overcome the restriction of the limited index

#168795 - $15.00 USD Received 17 May 2012; revised 18 Jun 2012; accepted 21 Jun 2012; published 25 Jun 2012

contrast in a fully-clad chalcogenide membrane (the refractive index of $Ge_{11.5}As_{24}Se_{64.5}$ is ~2,65 at λ = 1550 nm), we have designed a hetero-structure cavity that supports high Q resonances even when the PhC is completely embedded in a cladding with the index of silica. According to our simulations an intrinsic Q-factor (Q_v) of over 20 million could be achieved using our design. We successfully fabricated PhC hetero-structure resonators achieving Q_v of >7.5 x 10^5 which compares favorably with the value of 1.7 x 10^6 predicted from modeling of an ideal structure. Thus, we have demonstrated that it is possible to obtain high-Q cavities with a fully clad chalcogenide PhC leading to a reduced thermal nonlinearity that should make observation of ultra-fast Kerr nonlinear bistable switching possible.

2. Design of the PhC waveguide

Hetero-structure PhC cavities utilize the frequency shift between two guided modes of different waveguides produced by varying the lattice constant along a waveguide [16]. In order to obtain a geometry that potentially leads to a high Q-factor cavity, we first need to analyze the dispersion properties of the PhC waveguides in which the cavity will be created. The plane wave expansion method was used to calculate the band gap and guided modes of a W1 waveguide (Fig. 1) [1–3]. For a symmetric cladding we consider only the TE-like modes in which the electric field in the centre of the PhC slab is polarized in the plane of the slab. The nominal PhC parameters were a hole radius of 130 nm, a lattice period of 450 nm, and a slab thickness of 480 nm, slab index of 2.65 and cladding index 1.44. The hole size and slab thickness were fixed throughout the study, while the lattice constant in the direction parallel to the waveguide axis was used to define a hetero-structure that forms the cavity.

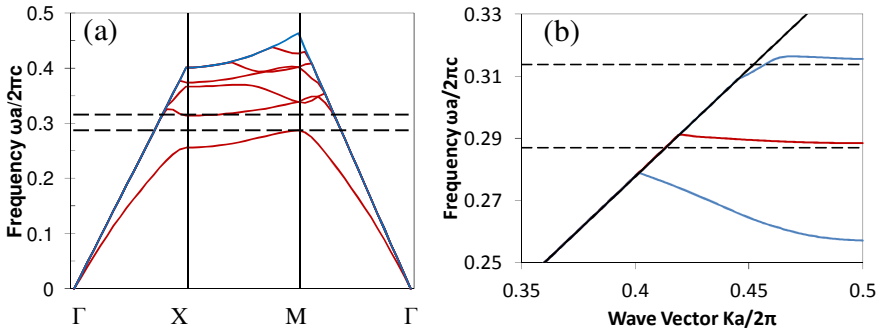

Fig. 1. (a) The calculated band structure for a $Ge_{11.5}As_{24}Se_{64.5}$ 2D photonic crystal slab with index 2.65 fully embedded in a silica cladding with index 1.44. Other parameters are given in the text. (b). Guided modes of a W1 waveguide (red) embedded in the PhC lattice of Fig. 1(a). The location of the bandgap of the photonic crystal is indicated by the horizontal dotted lines. The blue lines represent the edge of the slab bands of the PhC waveguide [2].

As shown in Fig. 1(a), the even mode exhibits a band gap between normalized frequencies of $\omega a/2\pi c = 0.286$ and $\omega a/2\pi c = 0.314$, where a is the lattice constant of photonic crystal. The guided modes for a W1 waveguide in this structure are shown in Fig. 1(b). Here we focus on the red curve that represents the lowest order even mode of the waveguide and lies within the bandgap defined by the blue curves and below the light line in black. Figure 1(b) shows that the bandwidth over which guidance can be obtained is only 0.78% of the central frequency, corresponding to 12nm at a wavelength of 1550nm. Such a narrow mode bandwidth would be very sensitive to fabrication imperfections, and would likely result in relatively high scattering losses to radiation states above the light line.

In order to create a high-Q resonant cavity within an embedded structure, we need to find a method to broaden the bandwidth of the guided mode of the photonic crystal waveguide. In silicon PhCs, a narrower waveguide has been shown to broaden the bandwidth of the guided modes [32] and hence we explored that approach. For our chalcogenide PhC, we found that if

#168795 - $15.00 USD Received 17 May 2012; revised 18 Jun 2012; accepted 21 Jun 2012; published 25 Jun 2012

the waveguide width was reduced down to W0.52~W0.58, the bandwidth for the guided even mode increased substantially as shown in Fig. 2(a). W0.58, W0.56, W0.54 and W0.52 waveguides in fact exhibit bandwidths of 2.8%, 2.5%, 2.1% and 1.8%, respectively, corresponding to values ranging from 28nm to 43nm which should be sufficient to reduce radiation losses and potentially allow high-Q values to be achieved. However, if the waveguide width was larger than W0.58, the frequencies of the guided modes drop to the point where they fall outside the band gap of the photonic crystal. An example is shown for W0.7 in Fig. 2(a). Moreover, for W-values above W0.7, the guided mode disappears into the bottom slab bands and a new guided mode emerges from the top, examples being W0.8 and W1 waveguides (Fig. 2(a)). As for the case of the W1 waveguide, the dispersion for the W0.8 waveguide is very flat which will prevent high-Q from being obtained. As a result, we choose a width of W0.54 which has both a broad bandwidth and is fully confined inside the band gap.

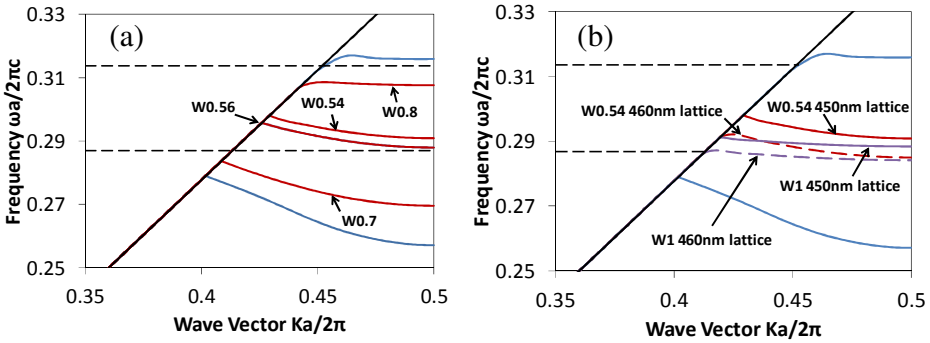

Fig. 2. (a): Guided modes for waveguide with different W-values (red) embedded in the PhC lattice of Fig. 1(a). (b): a comparison of the dispersion for the modes of both W1 and W0.54 waveguides that demonstrates the increased bandwidth achieved using the W0.54 structure. The dispersion curves are shown for two structures whose lattice constant differs by 10nm. The location of the bandgap of the photonic crystal is indicated by the horizontal dotted lines. The blue lines represent the edge of the slab bands of the PhC waveguide [2].

3. Performance of a simple hetero-structure cavity

We next needed to design and optimize a PhC hetero-structure cavity in the PhC waveguide. Firstly we concentrated on a simple hetero-structure where the lattice constant, a_m, of the mirror sections was changed in a step-wise manner from the lattice constant of the cavity, a_c. Figure 2(b) shows the guided modes for both W1 and W0.54 waveguides when the lattice constants differed by $\Delta a = a_c - a_m = 10$nm. As is evident, reducing the lattice constant shifts the waveguide mode to higher frequencies creating a narrow frequency range where a propagating mode is supported in one waveguide, but not the other. The mirrors are made from the waveguides with the smaller lattice constant, that is $a_m < a_c$. From Fig. 2(b) we can see that the guided mode of the W1 waveguide in the cavity with a_c = 460nm falls completely outside the band gap of the PhC and this leads to weak confinement in the horizontal direction. In fact the Q_v calculated using 3D FDTD simulations for this cavity was typically 8000. Even for the W0.54 waveguide a portion of guided mode in the cavity lies outside the band gap and this suggests that Q_v could be improved by fine-tuning the lattice constants so that the dispersion curve is moved completely within the band-gap. We will return to this point later.

In addition to the Q-factor, the mode volume V is another important parameter for a resonant cavity. It defines the volume over which the resonance extends and determines the light intensity inside the cavity and the minimum power required for switching. The mode volume is often represented in terms of the normalized mode volume $V_{norm} = n^3V/\lambda^3$ where λ is the wavelength of resonance and n the refractive index of the material [15, 17]. As both Q-

#168795 - $15.00 USD Received 17 May 2012; revised 18 Jun 2012; accepted 21 Jun 2012; published 25 Jun 2012

factor and V_{norm} determine the light intensity resonating in the cavity, Q_v/V_{norm} is routinely used to quantify resonant cavities. Accurate calculations of the cavity modes properties for very high Q cavities are numerically challenging and require significant computing resources. The numerical results in the remainder of this paper were calculated using a commercial 3D finite-difference-time-domain package (RSoft) running on a computing cluster.

Figure 3(a) shows a schematic of a W0.54 waveguide containing a hetero-structure cavity with a_c = 460nm and a_m = 450nm. Figure 3(b) shows the E_z electric field distribution of the resonant mode of such a cavity 8 lattice periods long whilst Fig. 3(c) plots Q_v and V_{norm} as a function of the cavity length (in lattice periods). Both the intrinsic Q and the mode volume first decrease for cavity lengths between 2 to 6 lattice periods long and then start to rise as the length increases further. For 24 lattice periods Q_v exceeds 10^6 and the mode volume reaches $3.5 \cdot \lambda^3/n^3$. This relatively small volume is achievable because the resonant cavity is formed from a very narrow waveguide even though it is quite long. The mode volume scales only slowly with cavity length whilst Q_v increases rapidly suggesting that the energy confinement improves as the cavity gets longer. In particular, increasing the cavity length reduces the spectrum of the mode in k-space and this has the effect of reducing the leakage into directions that fall outside the bandgap. From Fig. 3(d), we can see that the Q_v/V_{norm} reflects the trends in Q-factor and mode volume and a value of 2.94 x 10^5 is achieved for 24 lattice periods.

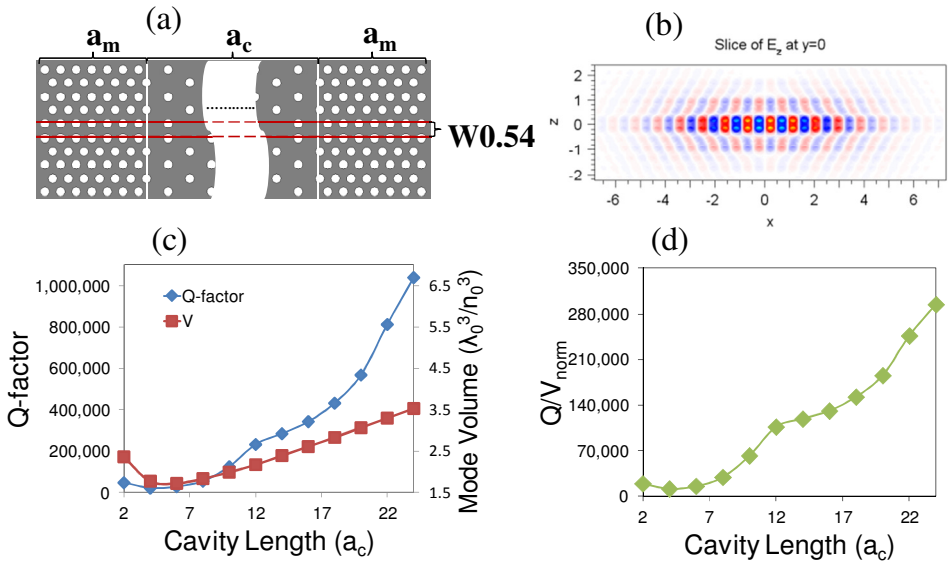

Fig. 3. (a) Diagram for W0.54 waveguide and hetero-structure with a stepped mirror. a_c = 460nm, a_m = 450nm. (b) The profile of E_z field of the resonant mode in the cavity. (c) Cavity Q factor (red) and normalized mode volume V_{norm} (blue) calculated as a function of cavity length. (d) Q/V_{norm} as a function of cavity length in lattice periods.

So far we have discussed the intrinsic Q-factor of the resonator achieved with complete confinement by semi-infinite mirrors at each end of the cavity. In a real device, light must be coupled in and out of the cavity either through the mirrors (end-coupling) or via evanescent coupling from a separate waveguide positioned parallel to the cavity (side-coupling). Thus the Q is reduced due to loading of the cavity by the coupling losses. The loaded Q-factor, Q_{total}, is determined by the coupling efficiency and can be represented as shown below using temporal coupled mode theory [3, 17]:

$$T_{end-coupled} = \frac{(Q_v - Q_{total})^2}{(Q_v)^2}, \qquad (1a)$$

#168795 - $15.00 USD Received 17 May 2012; revised 18 Jun 2012; accepted 21 Jun 2012; published 25 Jun 2012

$$T_{side-coupled} = \frac{(Q_{total})^2}{(Q_v)^2}, \tag{1b}$$

where $T_{end\text{-}coupled\,/\,side\text{-}coupled}$ is the transmission from the input to the output waveguide. In order to design the cavities, we calculated Q_{total} and T for the end-coupling geometry for mirrors of different lengths for a 24 period long cavity for which $Q_v > 10^6$. As shown in Fig. 4, Q_{total} increases as more lattice periods are added to the mirrors whilst the transmission decreases. With mirrors 14 lattice periods long, Q_{total} ~Q_v but the transmission has dropped nearly to zero.

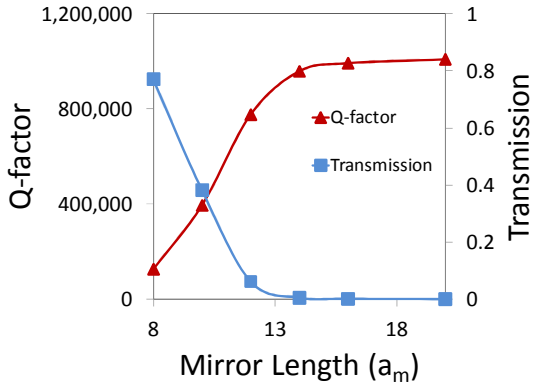

Fig. 4. The loaded Q-factor (red) and transmission (blue) of an end-coupled cavity as a function of the number of mirror length, for a 24 lattice period long cavity.

Figure 4 demonstrates that although we achieved an intrinsic Q_v of over 1 million, this is not accessible since good transmission efficiency is also required in a real resonator. This makes it important to investigate where we can improve the design to achieve an even higher value of Q_v thus allowing to very large Q_{total} and large transmission simultaneously.

4. Improving the cavity design

A graded mirror structure can improve the reflectivity of the mirrors by smoothing the effective index change at the end of the cavity and is, therefore, a promising method for enhancing Q_v in hetero-structure photonic crystals [16]. Two different types of graded mirrors were, therefore, investigated and these are shown schematically in Figs. 5(a) and 5(b). They correspond to the use of either one or two graded sections with lattice constants intermediate between the cavity and the mirrors. Using a graded mirror consisting of a single section two lattice periods long (Fig. 5(a)), Q_v could be increased to 2.5 x 10^6 for the 24 period long cavity. This is demonstrated in Fig. 5(c) where we plot Q_v and mode volume as a function of the lattice shift, $\Delta a_1 = a_1 - a_m$, between the intermediate section and the mirror.

#168795 - $15.00 USD Received 17 May 2012; revised 18 Jun 2012; accepted 21 Jun 2012; published 25 Jun 2012

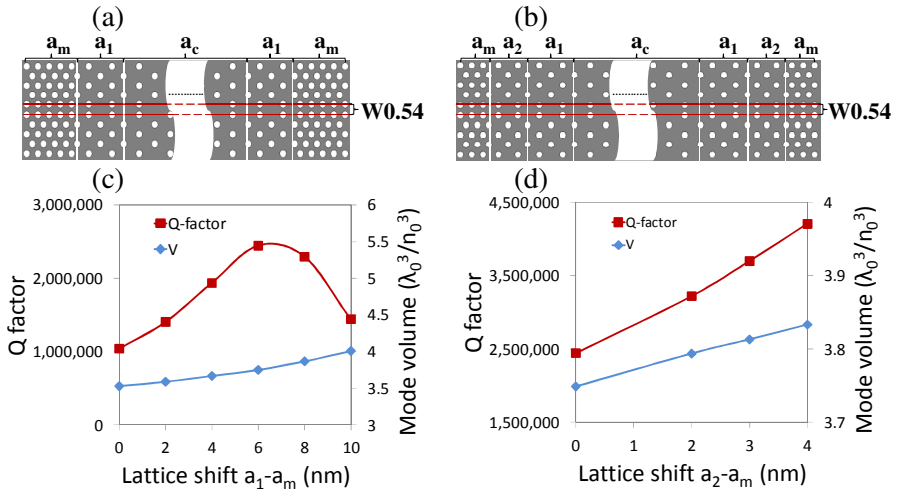

Fig. 5. (a) and (c) The Q factor (red) and mode volume (blue) as a function of shifted lattice constant $\Delta a_1 = a_1 - a_m$ with two periods graded mirror section. (b) and (d) The Q factor (red) and mode volume (blue) as a function of shift lattice constant $\Delta a_2 = a_2 - a_m$ with four periods graded mirror section. For (b) and (d), the first two periods of graded mirror has a fixed lattice shift Δa_1 = 6nm and Δa_2 are varied for the 3rd and 4th periods.

By increasing the number of intermediate sections to two, each two lattice periods long (Fig. 5(b)), Q_v was further enhanced to over 4 x 10^6. In this example (Fig. 5(d)) the lattice shift of the section closest to the cavity was fixed at Δa_1 = 6nm, and the shift for the first section, $\Delta a_2 = a_2 - a_m$, was varied from 0 to 4nm. These results show that at least 4 times improvement of the Q_v could be obtained simply by using graded mirrors.

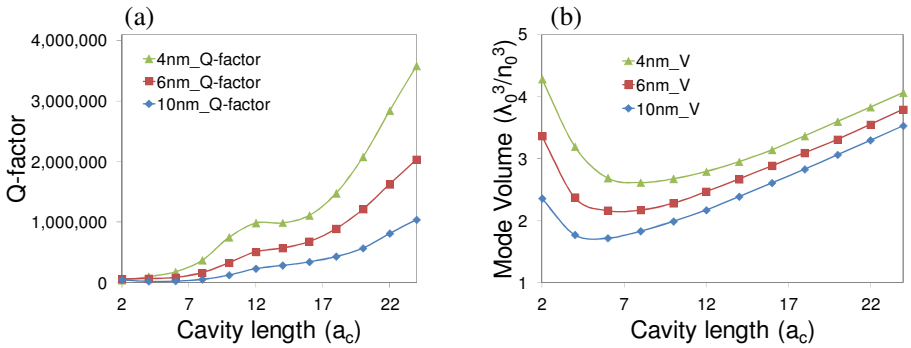

Fig. 6. (a) The Q-factor and (b) mode volume as a function of the cavity length for a hetero-structure cavity employing step mirrors as in Fig. 3(a). The different curves in each figure correspond to different lattice constant shifts, Δa, between the cavity and the mirrors.

As we noted earlier, for all the designs presented so far, part of the guided mode of the cavity lies outside the bandgap of the photonic crystal. Whilst this does not appear to prevent high-Q being obtained in sufficiently long cavities, higher Q_v would be expected if the guided modes were moved completely inside the bandgap. This can be achieved, for example, by reducing the lattice constant shift of the cavity relative to the mirrors (i.e. reducing Δa). Reducing Δa to 4nm in fact moves the guided mode of the cavity completely inside the bandgap. The effect on the cavity Q_v is demonstrated in Fig. 6 where we compare the Q_v and mode volumes for a simple hetero-structure cavity with different length for Δa = 10nm, 6nm or 4nm. Using a 6nm shift more than doubles the Q-factor whilst for a 4nm shift it increases

#168795 - $15.00 USD Received 17 May 2012; revised 18 Jun 2012; accepted 21 Jun 2012; published 25 Jun 2012

more than 3 times. At the same time the mode volume does not increase significantly especially if the cavity is more than about 12 periods long.

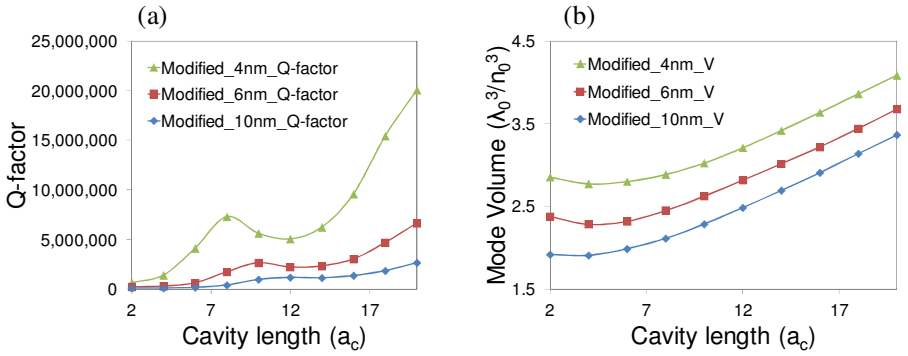

Fig. 7. (a) The Q-factor and (b) mode volume as a function of the cavity length for a hetero-structure cavity employing graded mirrors. The different curves in each figure correspond to different lattice constant shifts, Δa, between the cavity and the mirrors.

By adding graded mirrors the Q-factor increases again as demonstrated in Fig. 7. For a 24 period long cavity with a Δa = 4nm, Q_v over 2 x 10^7 is then predicted. For this design the graded mirror comprised two intermediate sections each two lattice periods long. The first intermediate section (closest to the cavity) had $\Delta a_2 \approx 0.6\ \Delta a$ and the second section $\Delta a_1 = 0.4\ \Delta a$. This leads to a large enough Q_v to achieve a very high Q_{total} (>10^6) as well as efficient transmission. From these calculations it would appear that there is no impediment, in principle, to achieving high-Q cavities in a fully embedded chalcogenide photonic crystal although in practice imperfections introduced during fabrication will create an upper limit to Q_v.

From Figs. 3, 6 and 7, we notice that the Q-factor always increases with the cavity length much faster than mode volume. From mode patterns such as Fig. 3(b), it is clear that the field always extends outside the boundaries of the waveguide. As indicated earlier, for cavity designs where the mode is close to or intercepts the band edge of the photonic crystal, this can enhance leakage from the cavity to k-vectors weakly confined by the lattice. However, as the cavity length is increased the confinement improves which reduces the leakage increasing Q_v. Furthermore, Q_v does not increase monotonically with length but exhibits modulations at lengths around 8~12 periods. This is caused by our choice of a fixed mirror design that produces a specific phase response in reflection and this interferes with the phase of the wave in the cavity. When the reflection is in phase with the wave in the cavity, maximum reflectivity is achieved resulting in a local maximum in Q_v whilst when out of phase Q_v drops to a local minimum.

Another important property of a fully clad resonant cavity is its resistance to refractive index mismatch between the silica substrate and the material used as a top cladding. Since it is difficult to fill the small holes of the PhC with silica, we intended to use either a UV-curable polymer coating applied as a liquid or a refractive index matching oil as the top cladding. As a result, the refractive index of the top cladding might differ from that of the silica substrate and it is important to know what refractive index mismatch can be tolerated without seriously compromising Q_v. An example is shown in Fig. 8 where we plot Q_v as a function of the difference between the upper and substrate cladding indices for a cavity where $Q_v \approx 1.7 \times 10^6$. We assume here the lower cladding index is 1.44. As is apparent, the index of the upper cladding should be within ± 0.01 of this value to maintain the Q_v at about 90% of its maximum, although an index error of ± 0.04 of index still results in $Q_v \approx 8 \times 10^5$ which would be adequate for many applications; suggesting the structure is quite tolerant to index errors.

#168795 - $15.00 USD Received 17 May 2012; revised 18 Jun 2012; accepted 21 Jun 2012; published 25 Jun 2012

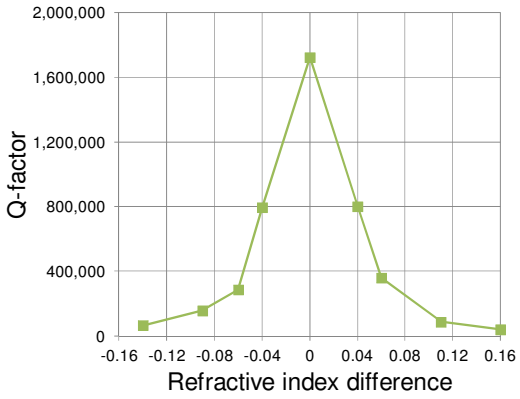

Fig. 8. The predicted variation of Q_v as a function of the mismatch in index between the top and bottom claddings.

5. Fabrication and characterization

Based on these numerical results, we fabricated a structure containing both end-coupled and side-coupled planar hetero-structure PhC cavities from a $Ge_{11.5}As_{24}Se_{64.5}$ film to the geometry shown in Fig. 9(a).

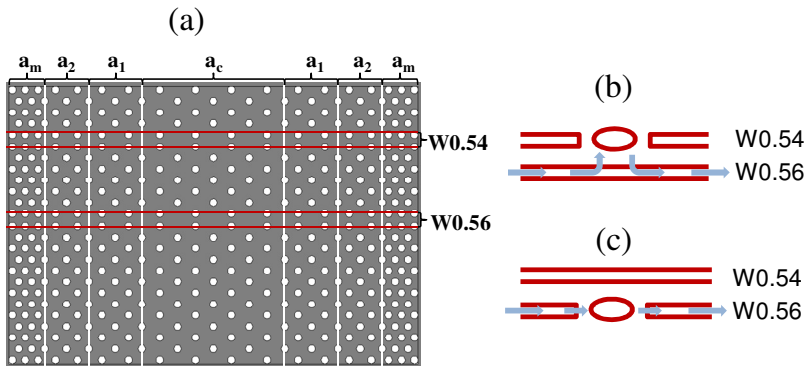

Fig. 9. (a) Diagram of the end-coupled (W0.56) and side-coupled (W0.54) cavities 8 lattice periods long incorporating a graded mirror structure with two intermediate sections. a_c, a_1, a_2 and a_m are the lattice constants for the cavity, the first intermediate section, the second intermediate section and the mirror respectively. A sketch showing energy flow in the side-coupled 9(b) and end-coupled 9(c) cavities respectively.

An end-coupled graded hetero-structure cavity 8 lattice periods long was formed in a W0.56 waveguide with the cavity lattice constant of a_c = 456nm and the mirror lattice constant of a_c = 450nm, that is $\Delta a = a_c - a_m$ = 6nm. The intermediate sections of the mirror had periods a_1 = 454nm, and a_2 = 452nm and were two period long. In the end-coupled geometry (Fig. 5(c)), light is coupled directly from an input waveguide into the resonant cavity through the first mirror and out-coupled through the second mirror to the output waveguide. The transmission from the input to the output waveguide at resonance is given by Eq. (1a). A side-coupled resonant cavity was incorporated in the design by placing a W0.54 waveguide 6 lattice periods away from the W0.56 waveguide as shown in Fig. 9(a). For this cavity, light is evanescently coupled from a propagating mode in the W0.56 waveguide into the resonant modes in the W0.54 cavity (Fig. 9(b)). The side-coupled cavity is better for determining the Q_v of the resonator from a measurement of the loaded Q_{total} and the depth of the transmission

#168795 - $15.00 USD Received 17 May 2012; revised 18 Jun 2012; accepted 21 Jun 2012; published 25 Jun 2012

dip via Eq. (1b). For this particular design, the theoretical Q_v for the cavity in the W0.54 waveguide was calculated to be ≈1.7 x 10^6.

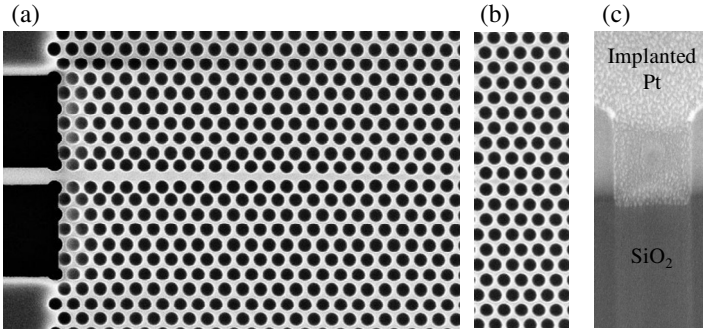

Fig. 10. SEM images of an end coupled $Ge_{11.5}$ photonic crystal. (a) and (b) The profile from top surface. (c) Cross section of holes cut by FIB and filled with Pt for imaging the side walls.

A photonic crystal conforming to this design was fabricated using the following process [33, 34]. First, a $Ge_{11.5}As_{24}Se_{64.5}$ film 480nm thick was thermally deposited onto an oxidized silicon wafer as a substrate. Then about 200nm of ZEP-520A was spin-coated onto the film as a positive resist for electron beam lithography. The photonic crystal was patterned into the ZEP using a Raith 150 electron beam lithography tool and wet developed. Inductively coupled plasma etching using CHF_3 gas was then used to transfer the photonic crystal pattern into the $Ge_{11.5}As_{24}Se_{64.5}$ glass. After etching and removal of the ZEP, a 2nm thick layer of Al_2O_3 was deposited by atomic layer deposition as a protective coating. According to the SEM images shown in Fig. 10, the resulting photonic crystal was of high quality with vertically etched surfaces (Fig. 10(c)). The left hand image in Fig. 10 shows that arrangement for coupling into the cavities which involved a tapered section from a W1 to W0.56 waveguide in the PhC and the connection to a nanowire creating an access waveguide that extended to the edge of the chip. After hand cleaving, a Cargille refractive liquid with an index of 1.45 (at 589nm) was added as the top cladding.

We initially probed the transmission of this structure using a broadband super-continuum light source, coupled into the end of the W0.56 PhC waveguide via the access waveguide. We recorded the transmission using an optical spectrum analyzer with a resolution of 0.01nm in order to locate the cavity resonances (Fig. 11(a)). Three resonances were apparent: those at 1594nm and 1605nm were due to the second and first modes of the side-coupled cavity (in the W0.54 waveguide), respectively whilst that at 1618nm was the first mode of the in-line cavity in the W0.56 waveguide. The drop in transmission at 1607nm shows the onset of the bandgap in the mirror sections of the W0.56 waveguide. The loaded Q-factor for the cavity at 1605.2nm was measured to be 1.2 x 10^5 using a tunable CW laser with a resolution of 1pm whilst those at 1594nm and 1605nm were lower at around 2.2 x 10^4 and 4.4 x 10^4 respectively. The resonance at 1605.2nm is shown (inverted) in Fig. 11(c) and was associated with a dip in the transmission 16dB deep (Fig. 11(b)) and a width of 13.3pm. The spectrum was fitted with a Lorentzian peak to obtain the spectral width, and by applying Eq. (1b), Q_v was estimated to be 7.6 x 10^5. This is the highest value ever reported for a chalcogenide photonic crystal with the intrinsic Q rivaling what has been achieved in silicon PhCs [16].

#168795 - $15.00 USD Received 17 May 2012; revised 18 Jun 2012; accepted 21 Jun 2012; published 25 Jun 2012

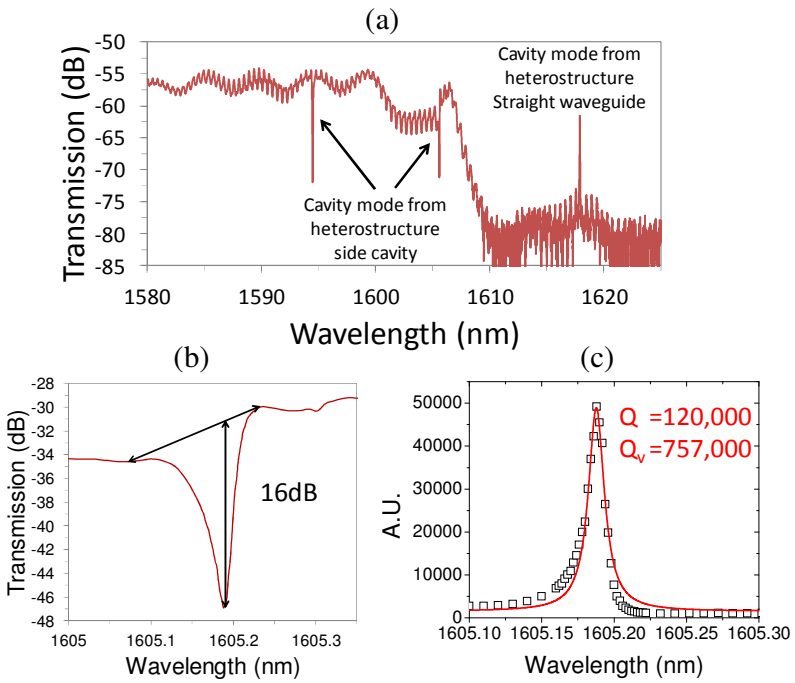

Fig. 11. (a) Optical transmission of the fully embedded $Ge_{11.5}As_{24}Se_{64.5}$ PhC measured using a supercontinuum source and OSA with a resolution of 0.01nm. Light was coupled into the W0.56 waveguide shown in Fig. 9. Three resonance peaks are apparent: two from the W0.54 side cavity at ≈1594nm and 1605nm and one from the W0.56 in-line cavity at ≈1618mn. (b) A scan of the 1605nm resonance using a tunable laser with 1pm resolution. (c) The same spectrum as (b); inverted and fitted to a Lorentzian curve. From these measurements the Q_v can be deduced to be 7.6 x 10^5.

4. Conclusions

We have shown that with careful design, high-Q micro-cavities can be produced in chalcogenide glass PhCs fully embedded in a silica cladding in spite of the low index contrast of only 1.21. Using a narrow W0.52-W0.58 waveguide extends the bandwidth of the guided mode within the bandgap reducing radiation losses that inevitably occur in the case of a W1 waveguide. In addition, fine-tuning the waveguide width and the lattice period offset allows the resonant mode in a hetero-structure cavity to be moved away from the edge of the photonic bandgap improving the confinement of light and hence the cavity Q_v. Using a W0.54 waveguide, intrinsic $Q_v > 10^7$ are possible in ideal structures.

To demonstrate the design we fabricated a hetero-structure cavity with graded mirrors to a design that that had a calculated intrinsic Q_v = 1.7 x 10^6. We determined the width and depth of a resonance for a loaded cavity side-coupled to a bus waveguide to be 1.2 x 10^5 and −16dB respectively. From these we could determine the Q_v of the fabricated resonator to be ≈7.6 x 10^5. The difference between the measured and predicted values is almost certainly attributable to deviations in the structure from the ideal with possibly a contribution from index asymmetry between the silica under-cladding and the Cargille liquid upper-cladding at ≈1600nm. By increasing the mirror transmission for an end-coupled cavity, or moving the bus waveguide closer for the side-coupled cavity, this structure would be sufficient to achieve loaded Q's of ≈10,000 with a resonance >30dB deep which should support bi-stable Kerr switching on a timescale of several 10s of ps. Finally a real benefit of the embedded structure is its mechanical stability and the potential for athermal behavior. In the present structure the

#168795 - $15.00 USD Received 17 May 2012; revised 18 Jun 2012; accepted 21 Jun 2012; published 25 Jun 2012

thermo-optic coefficient of the oil used as a cladding was large and negative and, in fact, reversed the temperature dependence of the resonance frequency relative to the unclad glass. This suggests that zero temperature dependence is achievable if a suitable cladding can be found.

Acknowledgments

The research was conducted by the Australian Research Council Centre for Excellence for Ultrahigh bandwidth Devices for Optical Systems (project number CE110001018). The device fabrication was partially supported by the facilities of the Australian National Fabrication Facility (ANFF). The calculation was supported by the National Computational Infrastructure (NCI) National Facility.

#168795 - $15.00 USD Received 17 May 2012; revised 18 Jun 2012; accepted 21 Jun 2012; published 25 Jun 2012